J|A|C|S
ARTICLES
Published on Web 12/24/2003

Aligned Inclusion of Hemicyanine Dyes into Silica Zeolite Films for Second Harmonic Generation

Hyun Sung Kim,† Seung Mook Lee,‡ Kwang Ha,† Changsoo Jung,‡ Yun-Jo Lee,† Yu Sung Chun,† Doseok Kim,‡ Bum Ku Rhee,‡ and Kyung Byung Yoon*,†

Contribution from the Departments of Chemistry and Physics, Sogang University, Seoul 121-742, Korea

Received August 6, 2003; E-mail: yoonkb@ccs.sogang.ac.kr

Abstract: Silicalite-1 films (thickness = 400 nm) supported on both sides of glass plates (SL/G) were prepared, and hemicyanine dyes (HC-*n*) with different alkyl chain lengths (*n*, *n* = 3, 6, 9, 12, 15, 18, 22, and 24) were included into the silicalite-1 films by dipping SL/Gs into each methanol solution of HC-*n* (1 mM) for 1 d. The included numbers of HC-*n* per channel (N_C) generally decreased with increasing *n*; that is, they were 6.4, 23.1, 15.4, 8.2, 5.7, 3.5, 0.9, and 1.2 molecules per channel, respectively. The d_{33} value gradually increased with increasing *n* but decreased when $n > 18$; that is, they were 1.12, 0.50, 2.25, 3.59, 4.99, 5.30, 1.71, and 2.57 pm V^{-1}, respectively. However, d_{33}/N_C progressively increased with increasing *n*. The d_{31} values were ~100 times smaller than the corresponding d_{33} values, and the average d_{33}/d_{31} ratio was 109, which is higher than those of Langmuir−Blodgett (LB) films and poled polymers of nonlinear optical (NLO) dyes, by ~2−5 and ~30−50 times, respectively. The estimated average tilted angle of the dyes with respect to the channel direction was 7.7°, and the calculated average order parameter was 0.97, which is ~480 times higher than the values observed from poled polymers. The degree of uniform alignment (DUA) generally increased with increasing *n*. The progressive increase of both DUA and d_{33}/N_C with *n* is attributed to the increase in the tendency of HC-*n* to enter hydrophobic silicalite-1 channels with the hydrophobic alkyl chain first. A more than 134-fold increase in DUA was observed upon increasing *n* from 6 to 24. The DUA of HC-24 in the silicalite-1 film reached close to 1. Although the observed d_{33} values were lower than those of the LB films of NLO dyes due to very small dye densities of the silicalite films, this methodology bears a great potential to be developed into the methods for preparing practically viable NLO films.

Introduction

Although there are a large variety of dipolar organic nonlinear optical (NLO) dyes with high second-order hyperpolarizability constants (β values), most of their crystals are inactive for optical second harmonic generation (SHG) due to the strong tendency of the dyes to align centrosymmetrically within the crystals.[1,2] Furthermore, the methods developed for crystallizing the NLO dyes in acentric symmetries have been shown to be successful only in limited cases.[1−3] Efforts have therefore been directed at utilizing the NLO dyes as self-assembled mono- or multilayers[4−8] and polymer-NLO dye composite films[1,2,9−13] supported on optically transparent substrates. However, the disadvantages associated with the organic thin films of NLO dyes[1,2] have triggered scientists to search for other novel conceptual approaches in the use of the dipolar NLO dyes.

† Department of Chemistry.
‡ Department of Physics.

(1) Nalwa, H. S., Myata, S., Eds. *Nonlinear optics of organic molecules and polymers*; CRC: Florida, 1997.
(2) Gunter, P., Ed. *Nonlinear optical effects and materials*; Springer: Heidelberg, 2000.
(3) (a) Eaton, D. F.; Anderson, A. G.; Tam, W.; Wang, Y. *J. Am. Chem. Soc.* **1987**, *109*, 1886−1888. (b) Tam, W.; Eaton, D. F.; Calabrese, J. C.; Williams, I. D.; Wang, Y.; Anderson, A. G. *Chem. Mater.* **1989**, *1*, 128−140. (c) Wang, Y.; Eaton, D. F. *Chem. Phys. Lett.* **1985**, *120*, 441−444. (d) Tomaru, S.; Zembutsu, S.; Kawachi, M.; Kobayashi, M. *Chem. Commun.* **1984**, 1207−1208. (e) Weissbuch, I.; Lahav, M.; Leiserowitz, L.; Meredith, G. R.; Vanherzeele, H. *Chem. Mater.* **1989**, *1*, 114−118.
(4) Ashwell, G. J.; Hargreaves, R. C.; Baldwin, C. E.; Bahra, G. S.; Brown, C. R. *Nature* **1992**, *357*, 393−395.
(5) Katz, H. E.; Scheller, G.; Putvinski, T. M.; Schilling, M. L.; Wilson, W. L.; Chidsey, C. E. D. *Science* **1991**, *254*, 1485−1487.
(6) Kanis, D. R.; Ratner, M. A.; Marks, T. J. *Chem. Rev.* **1994**, *94*, 195−242.
(7) (a) Facchetti, A.; Abbotto, A.; Beverina, L.; van der Boom, M. E.; Dutta, P.; Evmenenko, G.; Pagani, G. A.; Marks, T. J. *Chem. Mater.* **2003**, *15*, 1064−1072. (b) Wang, G.; Zhu, P.; Marks, T. J.; Ketterson, J. B. *Appl. Phys. Lett.* **2002**, *81*, 2169−2171. (c) Milko, E.; van der Boom, M. E.; Evmenenko, G.; Marks, T. J. *Adv. Funct. Mater.* **2001**, *11*, 393−397. (d) Zhao, Y.-G.; Wu, A.; Lu, H. L.; Chang, S.; Lu, W.-K.; Ho, S. T. *Appl. Phys. Lett.* **2001**, *79*, 587−589. (e) Facchetti, A.; Abbotto, A.; Beverina, L.; van der Boom, M. E.; Dutta, P.; Evmenenko, G.; Marks, T. J.; Pagani, G. A. *Chem. Mater.* **2002**, *14*, 4996−5005. (f) Wostyn, K.; Binnemans, K.; Clays, K.; Persoons, A. *J. Phys. Chem. B* **2001**, *105*, 5169−5173. (g) Bénard, S.; Yu, P.; Audière, J. P.; Rivière, E.; Clément, R.; Guilhem, J.; Tchertanov, L.; Nakatani, K. *J. Am. Chem. Soc.* **2000**, *122*, 9444−9454. (h) Schwartz, H.; Mazor, R.; Khodorkovsky, V.; Shapiro, L.; Klung, J. T.; Kovalev, E.; Meshulam, G.; Berkovic, G.; Kotler, Z.; Efrima, S. *J. Phys. Chem. B* **2001**, *105*, 5914−5921. (i) Lin, S.; Meech, S. R. *Langmuir* **2000**, *16*, 2893−2898.
(8) (a) Yang, X.; McBranch, D.; Swanson, B.; Li, D. *Angew. Chem., Int. Ed. Engl.* **1996**, *35*, 538−560. (b) Huang, W.; Helvenston, M. *Langmuir* **1999**, *15*, 6510−6514.
(9) Dalton, L. R.; Harper, A. W.; Ghosn, R.; Steier, W. H.; Ziari, M.; Fetterman, H.; Shi, Y.; Mustacich, R. V.; Jen, A. K.-Y.; Shea, K. J. *Chem. Mater.* **1995**, *7*, 1060−1081.
(10) Marder, S. R.; Kippelen, B.; Jen, A. K.-Y.; Peyghambarian, N. *Nature* **1997**, *388*, 845−851.
(11) van der Boom, M. E. *Angew. Chem., Int. Ed. Engl.* **1996**, *41*, 3363−3366.
(12) Samyn, C.; Verbiest, T.; Persoons, A. *Macromol. Rapid Commun.* **2000**, *21*, 1−15.

Along this line, zeolites and the related nanoporous materials have been examined as the hosts for aligned inclusion of organic dipolar NLO dyes to explore novel organic−inorganic composite SHG materials.[14−22] Thus, Stucky and co-workers first reported that *para*-nitroaniline (PNA), 2-methyl-4-nitroaniline (MNA), 2-amino-4-nitropyridine, and the analogous compounds readily enter the straight channels of $AlPO_4$-5 [a noncentrosymmetric (*P*6*cc*) zeolite analogue having one-dimensional channels with a diameter of 0.8 nm], and the dye-incorporating $AlPO_4$-5 powders generate second harmonic (SH) with the intensity far exceeding that of quartz powders.[14,15]

Subsequent studies by Marlow, Caro, and their co-workers revealed that the SHG activity of the PNA-including $AlPO_4$-5 crystals arose as a result of the spontaneous inclusion of PNA into the channels of $AlPO_4$-5 with the nitro group first caused by the intrinsically higher affinity of the $AlPO_4$-5 channels to the nitro than to the amino group.[16] Because the sizes of the crystals far exceeded (such as 130 μm) the wavelength of the incident laser beam (1.064 μm), the polarization reversal that occurred at the center of each crystal did not affect the overall SHG activities of the dye-loaded $AlPO_4$-5 crystals. They also found that the $AlPO_4$-5 crystals loaded with 4-nitro-*N*,*N*-dimethylaniline[17] or (dimethylamino)benzonitrile[18] are active for SHG.

The MFI-type structures such as ZSM-5[19] and Sb-incorporating silicalite-1 (Sb-SL)[20] [centrosymmetric (*Pnma*) zeolites having a three-dimensional channel system consisting of straight 0.54 × 0.56 nm channels in one direction and sinusoidal 0.51 × 0.54 nm channels in the other direction perpendicular to the straight channels] have also been shown to be SHG active upon PNA loading. However, in the case of Sb-SL loaded with PNA, the SHG activity disappeared after several exposures to incident laser beams. Unlike ZSM-5 and Sb-SL which contain Al and Sb, respectively, in the framework, the closely related pure silica ZSM-12 [a centrosymmetric (*C*2/*c*) silica zeolite having one-dimensional channels with a diameter of 0.56 × 0.59 nm] did not show any SHG activity even after inclusion of PNA.[21] PNA-loaded MCM-41 (an amorphous silica having a hexagonal array of channels with a diameter of 2−8 nm) also showed a SHG activity that was comparable to that of potassium dihydrogen phosphate (KDP) powders whose d_{33} (a tensor component of the quadratic nonlinear susceptibility) is ∼3 pm V^{-1}.[22] For them to be SHG active, however, aging of the composite under humid air for several weeks was necessary, indicating the requirement of the water-assisted secondary reorganization of the included PNA molecules to give rise to a net bulk dipole moment.

Thus, the previous pioneering works have demonstrated the potential of zeolites and the related nanoporous materials to be developed into versatile inorganic hosts for preparation of practically viable organic−inorganic composite SHG materials. However, despite the fact that there are a large variety of dipolar organic NLO dyes with much higher β values ($>500 \times 10^{-30}$ esu), the previous studies have been limited to PNA and the analogous NLO dyes with relatively low β values ($\beta_{PNA} = (34.5 \pm 4) \times 10^{-30}$ esu)[23,24] and with two distinctively different terminals, to one of which the aforementioned $AlPO_4$-5, Sb-SL, and ZSM-5 channels happened to show a higher intrinsic preference. Furthermore, the examined zeolite forms have been limited to powders and very small single crystals that bear no practical applicability. It is therefore necessary to develop methods for including dipolar NLO dyes with higher β values into the zeolites in uniform orientations so that the previous pioneering efforts can bear fruit. Also, for practical viability, efforts should be directed at utilizing uniformly aligned zeolite films as hosts for the aligned inclusion of NLO dyes rather than small crystals and powders.

We now report a method for incorporating hemicyanine (HC) ($\beta \geq 770 \times 10^{-30}$ esu) with the *N*-alkyl pyridinium side first into the channels of uniformly aligned silicalite-1 films and that the HC-loaded silicalite-1 films show high SHG activities.

Experimental Section

We prepared silicalite-1 films supported on both sides of glass plates (SL/G) and a series of HCs with different alkyl chain lengths (HC-*n*, $n = 3$, 6, 9, 12, 15, 18, 22, and 24), on the basis of the hypothesis that slim, dipolar NLO dyes having a long hydrophobic tail will enter hydrophobic zeolite channels with the tail part first, leading to aligned inclusion of the NLO dyes into the channels.

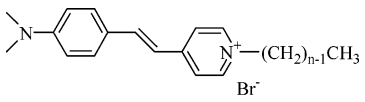

HC-*n*

n = 3, 6, 9, 12, 15, 18, 22, and 24

Subsequently, we incorporated the HC-*n* dyes into SL/Gs and investigated the effects of *n* on the included amounts of HC-*n* in each channel of SL/G, on the optical SH intensity ($I_{2\omega}$) of the resulting HC-*n*-including SL/G (HC-*n*-SL/G), and on the two tensor components of the quadratic nonlinear susceptibility, d_{31} and d_{33}, which were determined by Maker's fringe method.[25] The reason for choosing silicalite-1 films despite the fact that pure silica zeolites have never been employed as the hosts for aligned inclusion of NLO dyes is because they readily grow on glass with the straight channels (*b*-axis) orienting perpendicular to the glass plane and the channels are very hydrophobic. The measured d_{33} values were then compared with the maximum theoretical values. For the above, we also independently measured the absorption maximums (λ_{max}), the molar extinction coefficients (ϵ), and β values of HC-*n* dyes (β_{HC-n}).

(13) (a) Saadeh, H.; Yu, D.; Wang, L. M.; Yu, L. P. *J. Mater. Chem.* **1999**, *9*, 1865−1873. (b) Steire, W. H.; Chen, A.; Lee, S.-S.; Garner, S.; Zhang, H.; Chuyanov, V.; Dalton, L. R.; Wang, F.; Ren, A. S.; Zhang, C.; Todorova, G.; Harper, A.; Fetterman, H. R.; Chen, D.; Udupa, A.; Bhattacharya, D.; Tsap, B. *Chem. Phys.* **1999**, *245*, 487−506. (c) Jiang, H.; Kakkar, A. K. *J. Am. Chem. Soc.* **1999**, *121*, 3657−3665. (d) Dalton, L. R.; Steier, W. H.; Robinson, B. H.; Zhang, C.; Ren, A.; Garner, S.; Chen, A.; Londergan, T.; Irwin, L.; Carlson, B.; Fifield, L.; Phelan, G.; Kincaid, C.; Amend, J.; Jen, A. *J. Mater. Chem.* **1999**, *9*, 1905−1920.
(14) Cox, S. D.; Gier, T. E.; Stucky, G. D.; Bierlein, J. *J. Am. Chem. Soc.* **1988**, *110*, 2986−2987.
(15) (a) Cox, S. D.; Gier, T. E.; Stucky, G. D. *Chem. Mater.* **1990**, *2*, 609−619. (b) Cox, S. D.; Gier, T. E.; Stucky, G. D.; Bierlein, J. *Solid State Ionics* **1989**, *32*, 514−520.
(16) Marlow, F.; Wübbenhorst, M.; Caro, J. *J. Phys. Chem.* **1994**, *98*, 12315−12319.
(17) Caro, J.; Marlow, F.; Hoffmann, K.; Striebel, C.; Kornatowski, J.; Girnus, I.; Noack, M.; Kölsch, P. *Prog. Zeolite Microporous Mater.* **1997**, *105*, 2171−2178.
(18) Marlow, F.; Caro, J.; Werner, L.; Kornatowski, J.; Dähne, S. *J. Phys. Chem.* **1993**, *97*, 11286−11290.
(19) Werner, L.; Caro, J.; Finger, G.; Kornatowski, J. *Zeolites* **1992**, *12*, 658−663.
(20) Reck, G.; Marlow, F.; Kornatowski, J.; Hill, W.; Caro, J. *J. Phys. Chem.* **1996**, *100*, 1698−1704.
(21) Kinski, I.; Daniels, P.; Deroche, C.; Marler, B.; Gies, H. *Microporous Mesoporous Mater.* **2002**, *56*, 11−25.
(22) Kinski, I.; Gies, H.; Marlow, F. *Zeolites* **1997**, *19*, 375−381.
(23) Clays, K.; Persoons, A. *Phys. Rev. Lett.* **1991**, *66*, 2980−2983.
(24) Stähelin, M.; Burland, D. M.; Rice, J. E. *Chem. Phys. Lett.* **1992**, *191*, 245−250.
(25) (a) Maker, P. D.; Terhune, R. W.; Nisenoff, M.; Savage, C. M. *Phys. Rev. Lett.* **1962**, *8*, 21−22. (b) Herman, W. N.; Hayden, L. M. *J. Opt. Soc. Am. B* **1995**, *12*, 416−427.

Materials. A series of *n*-alkyl bromides ($C_nH_{2n+1}Br$) were purchased from TCI ($n = 3$, 6, 9, 12, 15, and 18) and Aldrich ($n = 22$) and were used as received. 1-Tetracosyl bromide (n-$C_{24}H_{49}Br$) was prepared from the corresponding alcohol (Aldrich) according to the following procedure. Triphenylphosphine (95 mg, 0.36 mmol) and carbontetrabromide (120 mg, 0.36 mmol) were sequentially introduced into a dichloromethane solution (50 mL) dissolved with 1-tetracosanol (60 mg, 0.17 mmol), and the mixture was stirred at room temperature for 12 h. The solvent was then removed by evacuation, and the produced 1-tetracosyl bromide was isolated from the reaction mixture by column chromatography. 4-[4-(Dimethylamino)styryl]pyridin (Aldrich), tetraethyl orthosilicate (TEOS, Acros), sodium aluminate ($NaAlO_2$, Kanto), and tetrapropylammonium hydroxide (TPAOH, Aldrich) were purchased and used as received. *n*-Octadecane and *n*-heptadecane were purchased from PolyScience Corp. and used as such. 4-Nitroaniline was purchased from Aldrich and used as such.

Preparation of 4-[4-(Dimethylamino)styryl]-1-*n*-alkylpyridinium Bromide (HC-*n*). The HC-*n* dyes were prepared by refluxing the acetonitrile solution (25 mL) of 4-[4-(dimethylamino)styryl]pyridin (1 mmol) and the corresponding 1-bromoalkane (1 mmol) for varying periods of time until the initially colorless solution turned dark red (for instance, it required 6 days for HC-18). The solvent from each reaction mixture was removed under vacuum. Ethyl acetate (100 mL) was introduced into the reaction flask containing the crude products, and the heterogeneous mixture was poured on top of a silica gel column. To remove nonreacted starting compounds, copious amounts of ethyl acetate were passed through the column until pure ethyl acetate was collected from the column. The residual red salt was separated from silica gel by passing copious amounts of methanol through the column, and by collecting the red methanol solution. The red product was isolated by evaporation of methanol. The product was redissolved into a minimum amount of methanol, and ether was added into the solution until the solution became cloudy. Upon keeping the cloudy solution at −20 °C overnight, microcrystals of HC-*n* precipitated at the bottom of the glass container, and they were collected by filtration. The yields were generally over 60%. Results of elemental analyses, matrix-assisted laser desorption ionization time-of-flight (MALDI-TOF) mass spectral data, ^1H and ^{13}C NMR spectra, and Fourier transform infrared (FT-IR) spectra are listed in the Supporting Information (Tables SI-1−4 and Figure SI-1). The above analytical results unambiguously confirmed the identities of HC-*n* dyes synthesized in this report.

Measurements of λ_{max} and ϵ of the Visible Band of HC-*n*. A series of 0.1 mM methanol solutions of HC-*n* were prepared. The UV−vis spectra of HC-*n* solutions were recorded using a matched pair of quartz cuvettes with optical path lengths of 1 cm. The absorbance values of the 0.02-mM solutions fell between 0.8 and 1. For each HC-*n* solution, the above measurement was repeated three times to deduce an average value of λ_{max} and ϵ, respectively.

Measurement of β_{HC-n} by Hyper Rayleigh Scattering (HRS). The β_{HC-n} values for $n = 6$, 12, and 22 were determined indirectly by comparison with that of PNA ($\beta_{PNA} = (34.5 \pm 4) \times 10^{-30}$ esu, in methanol at 1064 nm), which has been measured most reliably.[23,24] For this, the intensities of the incoherent SH radiations (I_{out}) of HC-*n* ($n = 6$, 12, and 22) and PNA were measured at various concentrations between 0.1 and 0.5 mM for HC-*n* and between 0.1 and 30 mM for PNA. The experimental setup is as follows. A rectangular quartz cuvette (path length = 1 cm) containing a methanol solution of a NLO dye was placed along the beam path of a mode-locked Nd:YAG laser beam (1064 nm, 10-Hz repetition rate, 40-ps pulse width with the intensity of I_{in}) 40 cm away from a focusing lens with the focal length of 50 cm. The cuvette was carefully positioned so that the beam can pass through the rightmost end of its front face to minimize absorption of the generated SH wave (532 nm) by the HC-*n* dyes whose absorption tails exceed 532 nm. The scattered incoherent SH radiation was collected with a lens facing the right-hand side of the cuvette, and the collected beam was passed through a monochromator to select only SH radiation and subsequently led to a photomultiplier tube (PMT). Figure 1A shows the HRS signal of PNA. The HC-*n* dyes produced very intense photoluminescence with the maximum at ~600 nm due to multiphoton absorption of the incident beam by the HC-*n* dyes as typically shown in Figure 1B for the case of HC-18. As a result, the HRS signals from HC-*n* dyes overlapped with the upper edge of an intense photoluminescence envelope as shown in Figure 1C. Accordingly, only the SH signals were extracted from the backgrounds by deconvolution.

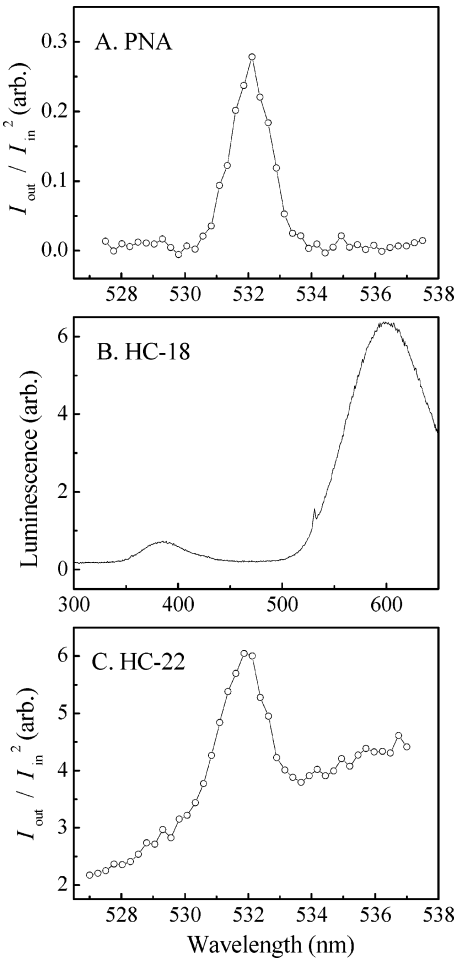

Figure 1. The HRS signal of the methanol solution of PNA (0.9 mM) (A), the photoluminescence spectrum of the methanol solution of HC-18 (B), and the HRS signal of the methanol solution of HC-22 (0.3 mM) overlapping with the upper edge of the intense photoluminescence envelope (C), arising from irradiation of each sample with 1064-nm laser pulses.

Preparation of Silicalite-1 Films. The growth of ZSM-5 and silicalite-1 films on porous substrates such as porous stainless steel, porous alumina, and porous Vycor glass disk and on nonporous substrates such as Teflon, silver, and silicon is well documented.[26] We therefore grew silicalite-1 and ZSM-5 films on flat glass by modification of the procedures and compositions of the synthesis gels described in the literature. For comparison, we also grew ZSM-5 films with several different Si/Al ratios on glass plates.

(26) (a) Auerbach, S. M., Carrado, K. A., Dutta, P. K., Eds. *Handbook of Zeolite Science and Technology*; Marcel Dekker: New York, 2003; Chapter 17 edited by Nair, S., Tsapatsis, M. (b) Yan, Y.; Davis, M. E.; Gavalas, G. R. *Ind. Eng. Chem. Res.* **1995**, *34*, 1652−1661. (c) Hedlund, J.; Mintova, S.; Sterte, J. *Microporous Mesoporous Mater.* **1999**, *28*, 185−194. (d) Tsikoyiannis, J. G.; Hagg, W. O. *Zeolites* **1992**, *12*, 126−130. (e) den Exter, M. J.; van Bekkum, H. V.; Rijn, C. J. M.; Kapteijn, F.; Moulijn, J. A.; Schellevis, H.; Beenakker, C. I. N. *Zeolites* **1997**, *19*, 13−20. (f) Wang, Z.; Yan, Y. *Chem. Mater.* **2001**, *13*, 1101−1107. (g) Xomeritakis, G.; Tsapatsis, M. *Chem. Mater.* **1999**, *11*, 875−878. (h) Ha, K.; Lee, Y.-J.; Chun, Y. S.; Park, Y. S.; Lee, G. S.; Yoon, K. B. *Adv. Mater.* **2001**, *13*, 594−596.

The growth of continuous silicalite-1 films on the glass plates was carried out by immersing five glass plates ($25 \times 70 \times 1$ mm^3) into the synthesis gel consisting of TEOS, TPAOH, and water in the mole ratio of 0.8:0.1:50, followed by heating at 140 °C for 5 h in a Teflon-lined autoclave. The synthesis gel was prepared by introducing TEOS (28.3 g) into a plastic beaker containing a TPAOH solution (150 mL, 0.11 M) with vigorous stirring. The gel was aged at room temperature for 12 h with vigorous stirring and was transferred to a Teflon-lined autoclave before immersion of glass plates. The obtained SL/Gs were thoroughly washed with copious amounts of water and dried in the atmosphere at room temperature. The resulting SL/Gs were cut into four pieces with the size of $\sim 25 \times 18 \times 1$ mm^3, and they were calcined at 450 °C for 12 h to remove TPA template prior to inclusion of NLO dyes. The thickness of each silicalite-1 film was monitored by taking the scanning electron microscope (SEM) images of the cross sections. Films with higher thickness ($\geq \sim 1$ μm) were also prepared either by increasing the immersion time in the synthesis gel or by re-immersing the glass plates coated with zeolite films into a fresh gel for a desired length of time.

ZSM-5 films with several different Si/Al ratios (50, 25, and 17) were also grown on glass plates by modification of the gel compositions. The gel compositions were TEOS:$NaAlO_2$:TPAOH:H_2O = 7:0.14:1:300, 7:0.28:1:300, and 7:0.42:1:300, respectively. The aging period and reaction temperature were fixed to be 5 h and 180 °C, respectively, and the reaction periods were 4, 4.3, and 5 h, respectively. The Si/Al ratios of the ZSM-5 films were determined with energy-dispersive X-ray analysis (EDX) of the films.

Inclusion of HC-*n* into SL/G and ZSM-5 Films. Into each vial (25 mL capacity) containing a methanol solution of different HC-*n* (10 mL, 1 mM) were added two SL/Gs, and the vial was kept at room temperature for a desired period of time such as 1 day, 1 week, or 3 weeks. After equilibration, the SL-Gs were removed from the solution, washed with copious amounts of fresh methanol, and dried in the air. For comparison of the SHG activities, SL/Gs from the same batch were used so that the characteristic factors of the film, such as the thickness, the degree of the coverage of the glass with silicalite film, the orientation of the film, and the morphology of the film, were as similar as possible. Furthermore, we took out a small portion from each SL/G and analyzed the characteristic factors of the films with SEM to ensure that the above factors are indeed similar from one sample to another and to discard any SL/Gs having significantly different factors from the average values.

Similarly, HC-18 was included into ZSM-5 films with Si/Al ratios of 50 and 25, respectively. Because of the poor film condition of ZSM-5 films with a Si/Al ratio of 17, inclusion of HC-18 into the films was not carried out.

Quantitative Analysis of the Included Amounts of HC-*n* in HC-*n*-SL/G. The HC-*n* dyes incorporated in SL/Gs were quantitatively analyzed according to the following procedure. A dilute aqueous solution of hydrofluoric acid (1 mL, a mixture of 0.2 mL of 49% HF and 0.8 mL of distilled deionized water) was introduced into a 50-mL plastic beaker containing a HC-*n*-SL/G. After gentle swirling of the mixture for 5 min at room temperature, the solution was neutralized by adding aqueous NaOH solution (1 mL, 5 M). Methanol (8 mL) was subsequently added into the neutral solution to ensure dissolution of all of the dye into the solution. After removal of the clean glass substrate from the solution, the solution was centrifuged to precipitate silica particles. The clean supernatant solution was decanted into one of the matched pair of quartz cells for a spectroscopic measurement. To increase accuracy in the quantitative analysis, we independently determined the molar extinction coefficient of each HC-*n* at a concentration similar to that of the extracted solution. For this, a mixed solvent with a composition similar to that of the extracted solution was prepared according to the following procedure. Freshly calcined silicalite (20 μg), 10 pieces of clean glass plates (18×25 mm^2), and hydrofluoric acid (10 mL consisting of 2 mL of 49% HF and 8 mL of distilled deionized water) were sequentially introduced into a 100-mL plastic beaker. After the beaker was swirled for 5 min, the solution was neutralized by adding aqueous NaOH solution (10 mL, 5 M). Methanol (80 mL) was subsequently added to the solution, and the clean supernatant solution was collected by centrifugation. Independently, a stock solution of HC-*n* in methanol was prepared by dissolving a known amount of HC-*n* (20−100 μg) in methanol (10 mL). An aliquot (1 mL) of the stock solution of HC-*n* was added into 100 mL of the above simulated solution, and the absorbance of the mixed solution was recorded. More aliquots were added into the simulated solution until the absorbance of the final solution became close to the one obtained from the HC-*n* solution extracted from HC-*n*-SL/G. We also extracted HC-22 from five HC-22-SL/Gs to increase the absorbance of the extracted solution as a means to increase accuracy in the quantitative analysis.

In estimating the degree of coverage of silicalite-1 film, the areas occupied by the empty spots and those covered by *a*-oriented twined crystals (the twined crystals whose *a*-axis are oriented perpendicular to the underlying basal crystal faces) were deducted from the total area. Those areas covered by second layers of silicalite-1 crystals were regarded as a single layer on the basis of the assumption that the channels in the upper and the bottom crystals are not aligned, and, as a result, inclusion of HC-*n* molecules is limited to the channels in the upper layers. For the above, a SEM image with a size of 32×21 μm^2 taken at a magnification of 4000 was photocopied onto a piece of paper so that the area of the SEM image became 32×21 cm^2, and the area covered by empty spots and *a*-oriented twined crystals was cut off using a sharp knife. By comparing the initial and final weights of the paper, the percentage of the area occupied by the *b*-oriented silicalite-1 film (the film whose *b*-axis is oriented perpendicular to the glass substrate) was deduced. The average percentage was deduced by repeating the above procedure for three different spots in a silicalite-1 film. Subsequently, given that the unit cell dimension of (010) plane is 2.007×1.342 nm^2 and each unit cell contains two straight channels,[27] the number of straight channels in each SL/G was deduced by dividing the area of each SL/G ($\sim 25 \times 18$ mm^2) by 2.007×1.342 nm^2 and taking into account the fact that a SL/G has two films.

Measurement of SH Intensity of HC-*n*-SL/G ($I_{2\omega}$) Relative to That of Quartz ($I_{2\omega}$ (quartz)). As an index matching fluid, a drop of dimethylsulfoxide (DMSO) was dropped onto each side of a HC-*n*-SL/G, respectively, and each side of the HC-*n*-SL/G was covered with a clean bare glass plate ($25 \times 18 \times 1$ mm^3). This was necessary to avoid scattering of the incident laser beam caused by the irregular thickness of the silicalite-1 films. A reference channel consisting of a beam splitter and a photodiode was used to compensate for the intensity fluctuations of the fundamental beam (1064 nm). The polarity of the fundamental laser beam was adjusted using a half-wave plate before it hit the sample. The electric field vector of the incident beam was either parallel (p-polarization) or perpendicular (s-polarization) to the plane of incidence. Only the p-polarized SH beam was made to enter a PMT by using a prism, a SH pass filter, and a polarizer. A HC-*n*-SL/G was mounted on the rotator coupled to a step motor. The output signals from the photodiode and PMT were detected as a function of an incident angle. A 3-mm-thick Y-cut quartz crystal (a piece of quartz plate whose plane is perpendicular to the crystalline *y*-axis and the thickness of the plate is 3 mm; see Figure SI-2 in the Supporting Information)[28] was used as a reference for determining the relative intensities of the SH signals ($I_{2\omega}/I_{2\omega}$ (quartz)) generated from the samples. The SH signals were collected from three different spots of a HC-*n*-SL/G, and the average intensity was taken.

(27) Baerlocher, Ch., Meier, W. M., Olson, D. H., Eds. *Atlas of zeolite framework types*, 5th revised ed.; Elsevier: New York, 2001; p 184.

(28) Quartz crystals generate SH along the *y*-axis. Therefore, a Y-cut quartz crystal is often used as a transmission SHG reference for Maker's fringe experiment. See: (a) Boyd, R. W. *Nonlinear Optics*, 2nd ed.; Academic: London, 2003; p 48. (b) Shen, Y. R. *The Principles of Nonlinear Optics*; Wiley: New York, 1988; p 101.

Comparison of the Affinities of Silicalite-1 Channels to *n*-Octadecane and HC-3. A methanol solution of *n*-octadecane (molecular weight = 254.5) was prepared by dissolving 12.73 mg of *n*-octadecane in 25 mL of methanol (2 mM). Freshly calcined silicalite-1 powder (50 mg) was introduced into 5 mL of the above solution. After the heterogeneous solution was allowed to equilibrate for 3 h at room temperature, the solution was filtered through a cotton-packed pipet. A known amount of *n*-heptadecane was added into the clear solution of *n*-octadecane as the internal standard, and the remaining amount of *n*-octadecane in the solution was determined by gas chromatography. The quantitative analysis of the included amount of HC-3 into silicalite-1 powder was similarly carried out by equilibrating 50 mg of freshly calcined silicalite-1 powder in a methanol solution of HC-3 (2 mM, 5 mL) for 3 h followed by measuring the absorbance of the supernatant solution on a UV−vis spectrophotometer.

Instrumentation. SEM images of zeolites and the zeolite-coated glass plates were obtained from a FE-SEM (Hitachi S-4300) at an acceleration voltage of 20 kV. A platinum/palladium alloy (in the ratio of 8 to 2) was deposited with a thickness of about 15 nm on top of the samples. The EDX analysis of the samples was carried out on a Horiba EX-220 Energy Dispersive X-ray Micro Analyzer (model: 6853-H) attached to the above FE-SEM. The X-ray diffraction patterns for the identification of the zeolite films were obtained from a Rigaku diffractometer (D/MAX-1C) with the monochromatic beam of Cu Kα. The UV−vis spectra of the samples were recorded on a Shimadzu UV-3101PC. FT-IR spectra were recorded on a Jasco FT/IR 620. ^{1}H and ^{13}C NMR spectra of the HC-*n* dyes were obtained from a Varian Jemini 500 NMR spectrometer. Elemental analyses of the HC-*n* dyes were performed on a Carlo-Erba EA1108. Mass spectral data were obtained from an Applied Biosystem MALDI TOF mass spectrometer (Proteomics Solution I Voyager-DE STR). Quantitative analysis of the included amount of *n*-octadecane into silicalite-1 was performed on a Hewlett-Packard 6890 series gas chromatograph equipped with a flame ionization detector. The fundamental laser pulses (1064 nm, 40-ps pulse width, and 10-Hz repetition rate) were generated from a Continuum PY61 mode-locked Nd:YAG laser.

Results and Discussion

Characteristics of SL/Gs and ZSM-5 Films. Silicalite-1 films readily grew on both sides of glass plates with their *b*-axes (straight channels) orienting perpendicular to the glass planes. Thus, as shown in Figure 2A, the diffraction lines appeared at a regular interval (2θ = 8.85, 17.8, 26.85, 34.85, and 45.55°) corresponding to the (0 2 0), (0 4 0), (0 6 0), (0 8 0), and (0 10 0) planes of the crystals. To make sure that the above regularly spaced X-ray diffraction pattern arises not due to the formation of an unknown zeolite film but due to the orientation of the silicalite-1 film with the *b*-axis perpendicular to the glass plane, the films were scraped off the glass plates and ground into fine powders to analyze the nature of the film. The X-ray diffraction pattern of the powders revealed that the film is indeed comprised of pure silicalite-1, as shown in the inset of Figure 2A. The SEM images shown in Figure 2B,C further confirmed that the silicalite-1 films are oriented with *b*-axes perpendicular to the substrate planes. The film thickness significantly varied depending on the batch. Although slightly, the thickness also varied within a film depending on the spot. The typical thicknesses were 400−500 nm, and the film thickness of the SL/G used in this report was ∼400 nm.

The quality of the film became inferior with an increase in the Al content in the gel (see Figure SI-3 in the Supporting Information). Consequently, the degree of the area of the glass plate covered by the *b*-oriented MFI-type film (with respect to the total area of the glass plate) decreased with an increase in the Al content; that is, they were 93%, 81%, and 57% for the films with Si/Al ratios of ∞, 50, and 25, respectively. Under the experimental conditions described in the Experimental Section, the film thicknesses of the ZSM-5 films were also ∼400 nm.

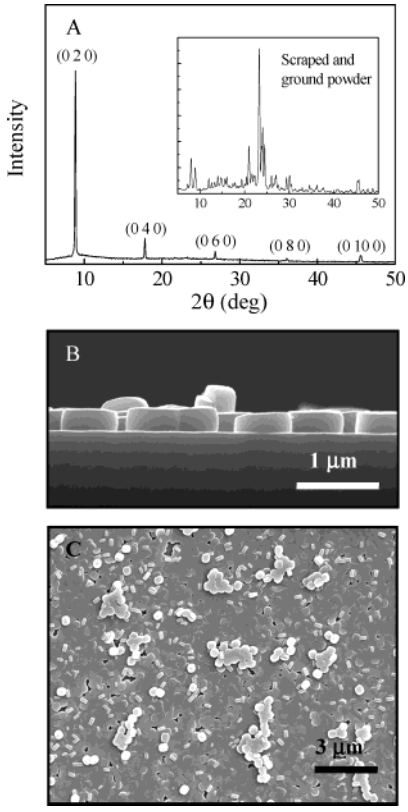

Figure 2. A typical X-ray diffraction pattern (A) and the SEM images (B, cross section; C, top view) of SL/G showing the alignment of the *b*-axis of the silicalite-1 film perpendicular to the glass plane. The inset in panel A shows the X-ray powder diffraction pattern of the silicalite-1 powder, which was obtained by finely grinding the film that was collected by scrapping the SL/G.

λ_{max} and ϵ of the HC-*n* Visible Band. The HC-*n* dyes were readily soluble in methanol, and the methanol solution showed a strong visible absorption band at ∼479 nm as shown in Figure 3A for HC-18. The determined ϵ values at ∼479 nm ranged from 39 515 to 45 160 (M^{-1} cm^{-1}) as listed in Table 1. As noticed, the tail length had almost no effect on the λ_{max} and ϵ, with a slight exception of HC-3, whose corresponding values are slightly smaller than those of the longer-tail homologues. It is therefore concluded that the hemicyanine head, 4-[4-(dimethylamino)styryl]pyridinium, is the part that determines the λ_{max} and ϵ values of the visible transition.

β_{HC-n} for n = 6, 12, and 22. The plots of the ratio between the SH intensity (I_{out}) and the square of the incident beam intensity (I_{in}^2), that is, I_{out}/I_{in}^2, with respect to the concentration was made for PNA and HC-*n* (n = 6, 12, and 22), respectively (Figure 4). In such a situation where a NLO dye is dissolved in a solvent, it is well established that I_{out}/I_{in}^2 can be expressed with the following:

$$I_{out}/I_{in}^{\ 2} = g[(\beta_{solvent})^2 C_{solvent} + (\beta_{dye})^2 C_{dye}] \times \exp[-(2\sigma_{in} l_{in} + \sigma_{out} l_{out}) C_{dye}] \quad (1)$$

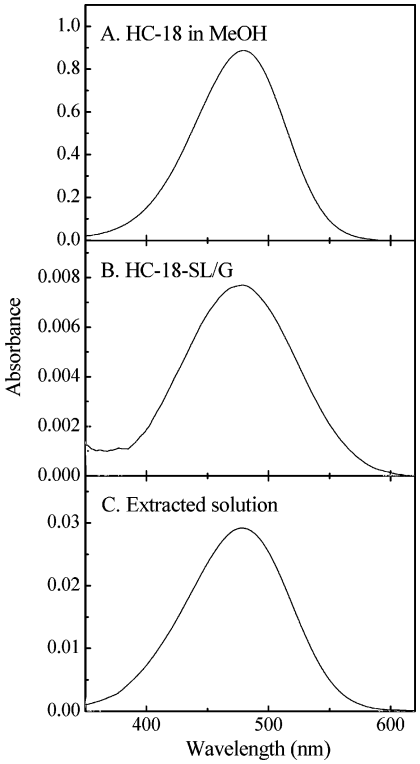

Figure 3. The UV−vis spectra of 0.02 mM HC-18 in methanol (A), HC-18-SL/G coated with DMSO as the refractive index matching fluid (B), and the aqueous methanol solution of HC-18 extracted from HC-18-SL/G (C).

where g denotes the geometric factor, $C_{solvent}$ and C_{dye} denote the concentration of the solvent and the NLO dye, respectively, $\beta_{solvent}$ and β_{dye} denote the β of the solvent and the NLO dye, respectively, σ_{in} and σ_{out} denote the absorption cross sections for incident beam and the SH, respectively, and l_{in} and l_{out} denote the path lengths of the incident beam and the generated SH within the solution, respectively. Based on eq 1, and the fact that the solvent does not absorb the incident beam, each relationship between I_{out}/I_{in}^2 and concentration shown in Figure 4 can be expressed with the following general formula:

$$y = (A + Bx)\exp(-Cx) \qquad (2)$$

where y and x denote I_{out}/I_w^2 and C_{dye}, respectively, and A, B, and C represent the parameters to be determined by curve fitting. The obtained parameters for each curve are listed in the inset of each panel of Figure 4. As noticed from the parameter values, the obtained values for A are essentially zero, consistent with the fact that the solvent used in this study (methanol) has a negligible SHG activity ($\beta_{solvent} = (0.69 \pm 0.07) \times 10^{-30}$ esu).[29] Therefore, by assigning the parameter A as zero, we determined that the β_{HC-n}/β_{PNA} ratios were expressed in terms of the parameter B as $(B_{HC-n}/B_{PNA})^{1/2}$, which were 22.3, 22.2, and 22.1 for $n = 6$, 12, and 22, respectively. The fact that the obtained ratios are very similar to each other indicates that the β_{HC-n} values are essentially identical regardless of n. By applying the reported value of β_{PNA} ($(34.5 \pm 4) \times 10^{-30}$ esu),[23,24] we determined the β_{HC-n} values to be $(765 \pm 89) \times 10^{-30}$ esu at 1064 nm. The above β_{HC-n} values are similar to the one reported by Ashwell et al., which is $(836 \pm 358) \times 10^{-30}$ esu at 1064 nm,[4] although the reported values in fact vary from 300×10^{-30} to 2300×10^{-30} esu at 1064 nm.[29−31]

Length of HC-*n* and Included Numbers of HC-*n* per Channel (N_C) of Silicalite-1 and ZSM-5 Films. The estimated maximum lengths of the HC-*n* dyes listed in Table 1 were estimated using the Chem Draw program. The increment was about 0.12 nm per methylene (CH_2) unit. The included number of each HC-*n* molecule per channel (N_C) after dipping a SL/G in a 1 mM solution of each HC-*n* for 1 d is also listed in Table 1. As noticed, N_C increased upon increasing n from 3 to 6 but rapidly decreased upon further increasing n. When the film thickness (~400 nm) was taken into account, even the occupancy of silicalite-1 channels by HC-6 with the largest N_C was only ~12% by length, which corresponds to 2 wt %. By the same analogy, the channel occupancies by HC-18, HC-22, and HC-24 were as small as 3%, 1%, and 1%, respectively, by length, which corresponds to 0.3%, 0.1%, and 0.1%, respectively, by weight. This indicates that only very small portions of silicalite-1 channels are occupied by the included HC-*n* molecules.

Interestingly, N_C of HC-18 into Na-ZSM-5 films increased with an increase in the Al content. For instance, whereas the N_C of HC-18 into an SL/G was 3.5 (Table 1), the corresponding numbers into Na-ZSM-5 films (Si/Al = 50 and 25) were 3.9 and 4.4, respectively. We attribute the above phenomenon to the ion exchange-aided incorporation of the positively charged HC-18 dye into the negatively charged channels by ion exchange of Na^+.

Irreversible Inclusion of HC-*n* into Silicalite-1 Channels. The colorless SL/Gs slowly picked up a pink hue upon immersion into methanol solutions of HC-*n*. The ready inclusion of HC-*n* into SL/Gs was confirmed by the UV−vis spectra of the DMSO-coated HC-*n*-SL/Gs, which were identical to the spectrum of HC-*n* in methanol, as typically shown in Figure 3B for HC-18. In the case of HC-6 with the largest N_C, we monitored the amount of inclusion of the dye into a SL/G with time (Figure 5). The result showed that the rate of inclusion was high before 4 h but decreased significantly after 4 h despite the fact that there are still enough rooms (>88%) in the channels.

Interestingly, if the dyes had once entered the silicalite channels, they never came out of the channels into solution. For instance, the intensities of the visible bands of HC-3-SL/G and HC-18-SL/G at 479 nm did not decrease even after keeping them in fresh methanol for 3 days, and the UV−vis spectra of the supernatant solutions also did not show any indication of leaching of HC-3 and HC-18 from silicalite-1 to methanol. The above result shows that the silicalite-1 channel has a very strong affinity toward HC-*n* dyes regardless of the chain length, indicating that inclusion of HC-*n* into the silicalite-1 channel is a nonequilibrium, irreversible process in methanol.

Although silicalite-1 does not have an ion-exchange capacity, it can be suspected that the HC-*n* dyes were included into the silicalite-1 channels as a result of ion exchange of the cations that might be present in the channels due to the presence of inadvertently introduced aluminum sites. To test such a possibility, we dispersed HC-6-SL/Gs into a 1 M aqueous solution of NaCl as a means to back exchange HC-6 with Na^+, because

(29) Duan, X.-M.; Okada, S.; Oikawa, H.; Matsuda, H.; Nakanishi, H. *Mol. Cryst. Liq. Cryst.* **1995**, *267*, 89−94.
(30) Marowsky, G.; Chi, L. F.; Möbius, D.; Steinhoff, R.; Shen, Y. R.; Dorsch, D.; Rieger, B. *Chem. Phys. Lett.* **1988**, *147*, 420−424.
(31) Bubeck, C.; Laschewsky, A.; Lupo, D.; Neher, D.; Ottenbreit, P.; Paulus, W.; Prass, W.; Ringsdorf, H.; Wegner, G. *Adv. Mater.* **1991**, *3*, 54−59.

Table 1. Effect of Alkyl Chain Length (*n*) on the Optical Properties of HC-*n* and the Amount of Inclusion into Silicalite-1 Film of 400-nm Thickness

n	λ_{max}[a]	ϵ[b]	β[c]	length[d]	*N* (×10^{14})[e]	N_C[f]	I_{pp}[g]	I_{sp} (×10^{-4})[g]	d_{33}[h]	d_{31}[h]	d_{33}/d_{31}	d_{33}/N_C	*s*[i]	DUA[j]
3	475.5	39 515		1.7	4.64	6.4	0.3		1.12			0.18		0.08[k]
6	479.0	43 355	769 (±89)	2.1	15.56	23.1	0.1		0.50			0.02		0.01[k]
9	479.0	43 775		2.4	10.37	15.4	1.6	0.5	2.25	0.02	113	0.15	0.97	0.09
12	480.0	42 460	766 (±89)	2.8	5.70	8.2	3.8	2.2	3.59	0.04	90	0.63	0.97	0.20
15	479.5	45 160		3.1	4.30	5.7	7.0	1.7	4.99	0.04	125	0.88	0.98	0.38
18	479.5	44 340		3.5	2.59	3.5	7.9	3.0	5.30	0.05	106	1.51	0.98	0.66
22	479.0	43 180	761 (±88)	4.0	0.61	0.9	0.9	0.4	1.71	0.02	86	1.90	0.97	0.91
24	479.0	42 320		4.2	0.88	1.2	1.9	0.9	2.57	0.03	86	2.14	0.97	0.95

[a] In nm. [b] Molar extinction coefficient in MeOH, M^{-1} cm^{-1}. [c] $\times 30^{-30}$ esu at 1064 nm in methanol. [d] In nm. [e] The total number of HC-*n* in a SL/G. [f] Number of HC-*n* in each 400-nm long channel of silicalite-1 film. [g] In % with respect to that of a Y-cut 3-mm-thick quartz crystal. [h] In pm V^{-1}. [i] The order parameter. [j] The degree of uniform alignment of HC-*n*, defined by the experimental-to-theoretical ratio of d_{33} values, $d_{33}(E)/d_{33}(T)$. [k] The average orientational angle ($\theta = 7.7°$) was taken to derive the theoretical d_{33} values.

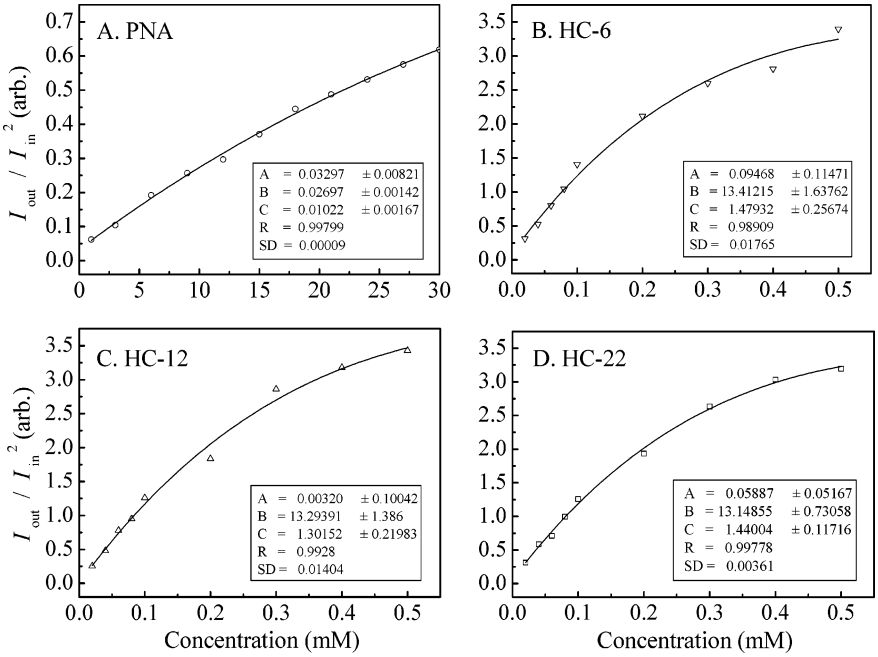

Figure 4. The plots of the intensities of the incoherent SH radiations (I_{out}) of PNA (A) and HC-6 (B), HC-12 (C), and HC-22 (D) with respect to the concentrations of the dye.

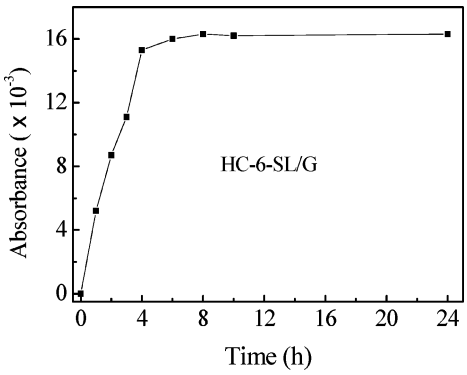

Figure 5. Change of the absorbance of HC-6-SL/G at 479 nm with time upon immersion of a SL/G into the methanol solution of HC-6 (1 mM).

the cationic dye has some solubility in water. However, the UV−vis analysis of the supernatant solution confirmed that HC-6 never came out of the silicalite film into the solution even after stirring the solution for 24 h at room temperature. Similarly, the HC-*n*-SL/Gs ($n = 6$, 18, and 22) were also immersed in a 1 M methanol solution of $NaClO_4$ for 24 h with an intention to back exchange HC-*n* with Na^+ in methanol in which the dyes are quite soluble. In this case again, the UV−vis analyses of the supernatant solutions showed that Na^+ ion does not induce extraction of HC-*n* ($n = 6$, 18, and 22) from the silicalite matrix to the solution.

In contrast to the case of HC-*n*-SL/Gs, 29% of the included HC-18 was extracted from the ZSM-5 film (Si/Al = 50) to the solution upon immersion into 1 M $NaClO_4$ in methanol solution for 24 h. The result shows that most of the HC-*n* cations are included into ZSM-5 channels via ion exchange.

***$I_{2\omega}/I_{2\omega}$* (quartz), d_{33}, and d_{31} of HC-*n*-SL/G.** The relative SH intensities (expressed in % with respect to a Y-cut 3-mm-thick quartz) are more specifically expressed as I_{pp} and I_{sp}, depending on the polarization direction of the incident beam, where the former and the latter denote the intensities of p-polarized SH beams generated from the p- and s-polarized fundamental laser beam, respectively. The typical plot of I_{pp} and I_{sp} of HC-18-SL/G versus the angle of the incident beam (with respect to the surface normal) is shown in Figure 6A. All of the other HC-*n*-SL/Gs showed nearly identical profiles. The completely destructive interferences in the profiles indicate that the two silicalite-1 films on the opposite sides of glass plates are nearly identical. The average angles at which the maximum values of I_{pp} and I_{sp} appeared were 67.4° and 55.9°, respectively.

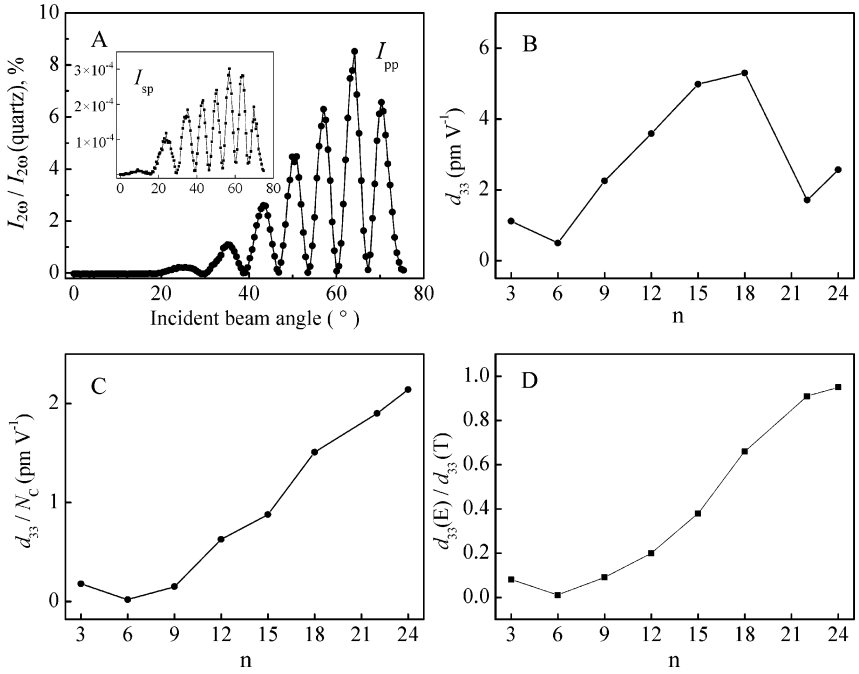

Figure 6. The plots of I_{pp} and I_{sp} (inset) of HC-18-SL/G (in %, with respect to the corresponding value of Y-cut 3-mm quartz) versus the angle of the incident beam (A) and the plots of d_{33} (B), d_{33}/N_C (C), and d_{33}(E)/d_{33}(T) (D) versus *n*.

The I_{pp} values ranged from 0.1% to 7.9%, while those of I_{sp} ranged from 0.4×10^{-4}% to 3.0×10^{-4}% (Table 1). The fact that the observed I_{pp} values are $\sim 10^4$ times larger than the I_{sp} values indicates that most of the dyes are positioned vertically with the long axis perpendicular to the glass plane, consistent with the aforementioned fact that most of the straight channels are oriented vertically with respect to the glass plane (Figure 2).

In general, the I_{pp} values of HC-*n*-SL/Gs were relatively smaller when $n \leq 6$ than when $n \geq 9$. In close relation to our work, Laeri and the co-workers reported that they observed SH signals from HC-2-loaded $ALPO_4$-5 crystals during their study of dye-incorporating zeolites as microlasers.[32] Although they did not report the quantitative SHG intensity, we expect that the SH intensity of the HC-2-loaded $ALPO_4$-5 crystals will be similar to the value of HC-3-SL/G. Although the difference was small, I_{pp} tended to decrease from 0.3 to 0.1 upon an increase in *n* from 3 to 6 despite the fact that N_c increased by ~4-fold. This result suggests that HC-6 enters silicalite-1 channels with a more random orientation than HC-3. However, I_{pp} progressively increased from 0.1% to 7.9% with an increase in *n* from 6 to 18, despite the progressive decrease in N_C. Interestingly, consistent with the sharp decrease of N_C, I_{pp} sharply decreased from 7.9% to 0.9% and 1.9% upon a further increase in *n* from 18 to 22 and to 24. Although small, the I_{sp} value also showed a trend similar to that of I_{pp} with increasing *n*.

The two tensor components of quadratic nonlinear susceptibility, d_{33} and d_{31} of HC-*n*-SL/Gs, were determined with Maker's fringe method[25] by comparing the experimentally observed relative I_{pp} and I_{sp} values with the intensity of a 3-mm-thick Y-cut quartz whose d_{11} is 0.3 pm V^{-1}. For this, 1.48 was used as the refractive index of silicalite-1 film based on the fact that DMSO can serve as a good index matching fluid, whose refractive index is 1.48 at 20 °C. The values are listed in Table 1 and graphically displayed in Figure 6B. Like I_{pp}, the d_{33} value initially decreased with an increase in *n* from 3 to 6, progressively increased with an increase in *n* from 6 to 18, but sharply decreased upon a further increase in *n*. However, d_{33}/N_C progressively increased with an increase in *n* (Table 1 and Figure 6C). The above results are highly reproducible even with other batches of SL/Gs. We propose that the above phenomenon arises as a result of the increase in the tendency of the HC-*n* molecule to enter the hydrophobic silicalite-1 channels with the hydrophobic tail first as the tail length increases.

The I_{pp} values observed from HC-18-loaded ZSM-5 films were 1.7% and 0.5%, respectively. Obviously, the I_{pp} values are much smaller than that of HC-18-SL/G (7.9%) despite the fact that N_C values are higher (3.9 and 4.4, respectively) in the ZSM-5 films than in SL/G (3.5) (vide supra). One obvious factor that caused the I_{pp} values to be lower than that of HC-18-SL/G is poorer coverage of glass plates with *b*-oriented ZSM-5 films. However, even after the lower coverage of ZSM-5 films (Si/Al = 50) on glass plates (81%) is taken into consideration, the resultant I_{pp} value is much lower than the expected value. This phenomenon is attributed to the increase in the degree of randomly oriented incorporation of HC-18 into the channels of ZSM-5 due to the increase in the hydrophilicity of the channels as a result of introduction of anionic centers in the framework and the charge-balancing cations. On the basis of the above observation, we rather concentrated on the aligned incorporation of HC-*n* dyes into SL/Gs.

Remarkably High Order Parameters of HC-*n* Dyes in SL/Gs. The calculated d_{33}/d_{31} ratios were always higher than 85, and the average was 109, which is ~2−5 times higher than those of Langmuir−Blodget (LB) films of nonlinear optical (NLO) dyes, which are ~30−50 times higher than those of poled polymers imbedded or grafted with NLO dyes, which are

(32) (a) Vietze, U.; Krauss, O.; Laeri, F.; Ihlein, G.; Schüth, F.; Limburg, B.; Abraham, M. *Phys. Rev. Lett.* **1998**, *81*, 4628−4631. (b) Braun, I.; Ihlein, G.; Laeri, F.; Nöckel, J. U.; Schulz-Ekloff, G.; Schüth, F.; Vietze, U.; Weiss, O.; Wöhrle, D. *Appl. Phys. B* **2000**, *70*, 335−343.

usually less than ~3.[1] The estimated average tilted angle of HC-*n* (θ) in the silicalite-1 channel based on the above very high average d_{33}/d_{31} ratio was 7.7°,[33] indicating that the long axes of the hemicyanine heads are tilted by the angle from the direction of the straight channels of silicalite-1 film (surface normal). The value is smaller than that of PNA in the straight channels of Sb-SL (11°),[20] and that of HC-18 in an LB film (18−40°).[4] The reason the θ value of the hemicyanine head is smaller than that of PNA in silicalite-1 channels is conceivable from the fact that the length of the former is much larger than the length of the latter.

The degree of orientational order of nonlinear chromophores can be quantified by the order parameter *s* which is expressed by eq 3.

$$s = [3\langle\cos^2\theta\rangle - 1]/2 \tag{3}$$

From the derived average θ of 7.7°,[33] the average order parameter (*s*) of HC-*n* in SL/Gs becomes 0.97, which is markedly higher than those of NLO dyes in poled polymers whose typical values are ~0.2.[1,2] We believe that *s* of HC-*n* in SL/Gs is the highest ever found among the SHG materials comprised of organic NLO dyes.

Marked Increase in the Degree of Uniform Alignment (DUA) of HC-*n* with Increasing *n*. We calculated the maximum theoretical d_{33} values of HC-*n*-SL/Gs based on eq 3 by taking N of HC-*n* in each HC-*n*-SL/G, the average value of β_{HC-n} (765×10^{-30} esu, or 3216×10^{-40} m^4 V^{-1}), the average tilted angle of HC-*n* dyes with respect to the surface normal (θ = 7.7°), and the microscopic local field correction $l = 1.40$ into account, and assuming that all of the included HC-*n* dyes were aligned with the alkyl tail part pointing to the glass substrate.

The calculated theoretical maximum d_{33} values [d_{33}(T)] were 14.40 (3), 70.71 (6), 24.48 (9), 18.13 (12), 13.31 (15), 8.03 (18), 1.88 (22), and 2.71 pm V^{-1} (24), respectively, for each *n* shown in the parentheses. The experimental-to-theoretical ratio of d_{33} [d_{33}(E)/d_{33}(T)] is defined as DUA. The DUA values are listed in Table 1 (last entry), and they are plotted against *n* in Figure 6D. As noticed, DUA generally increased with increasing *n*. We propose that such a phenomenon arises as a result of the increase in the tendency of the HC-*n* molecule to enter the hydrophobic silicalite-1 channels with the hydrophobic tail first as the tail length increases. The same proposal was made to account for the progressive increase of d_{33}/N_C (vide supra). In support of our proposal, it has been well established that silicalite-1 channels are hydrophobic and hence prefer alkanes to the relatively polar molecules such as alcohols.[34]

To be more certain, we also compared the included amounts of HC-3 and *n*-octadecane, respectively, into silicalite-1 powders after stirring for 3 h in each methanol solution under the consideration that HC-3 and *n*-octadecane represent the hemicyanine head and hydrophobic alkyl tail, respectively. Analyses revealed that the included amounts of HC-3 and *n*-octadecane were 0.01 mg (0.3 μmol) and 3.64 mg (143 μmol) per gram of silicalite-1, respectively, showing that the included number of *n*-octadecane was as much as 476 times larger than that of HC-3 within the period of 3 h, despite the fact that the estimated length of *n*-octadecane (2.4 nm) is longer than that of HC-3 (1.7 nm).

In close relation to the above, we also found that the initial rate of inclusion of HC-*n* into silicalite-1 powders from each dilute methanol solution of HC-*n* progressively increased with increasing *n* although the number of HC-*n* eventually included into SL/G after 15 h progressively decreased with increasing *n* as mentioned earlier. For example, when 20 mg of silicalite-1 powder (instead of SL/G) was immersed into each 10 mL aliquot of a dilute methanol solution of HC-*n* (0.02 mM) for 1 h at room temperature, the amounts of each HC-*n* included into silicalite-1 powders were 52, 45, 75, 98, 105, 143, 162, and 165 nmol per gram of silicalite-1 for $n = 3$, 6, 9, 12, 15, 18, 22, and 24, respectively.

The reversal of the order of included numbers of HC-*n* with time suggests that the intrachannel migration of HC-*n* becomes difficult as the alkyl chain length increases, unlike *n*-octadecane, presumably due to the increase in the effective width of HC-*n* as *n* increases. Coupled with the fact that the N_C values of HC-22 and 24 are close to 1, the increase in the difficulty of intrachannel diffusion of HC-*n* with increasing *n* made us suspect the possibility of HC-22 and HC-24 existing on the surface of the silicalite-1 films as monolayers by sticking their hydrophobic chains into the hydrophobic channels.

The comparison of the smallest and the largest DUA values, that is, 0.01 for $n = 6$ and 0.95 for $n = 24$, revealed the remarkable fact that the increase in *n* leads to as much as 95-fold increases in DUA. As noticed, the estimated DUA value for HC-24 came out close to 1. The value may be reduced to ~60% if the largest reported average β_{HC-n} value (2300×10^{-30} esu)[29−31] is used for the estimation of d_{33}(T). Despite the above uncertainty in obtaining the exact value of DUA, we believe that the d_{33}(T) value of HC-24 matches very closely with the experimentally observed value, considering the extreme difficulties in obtaining the absolute β values of NLO dyes and the exact number densities of the HC-*n* dyes in silicalite-1 films. Although the uncertainty has yet to be resolved, the fact that the increment in DUA becomes very small upon increasing *n* from 22 to 24 strongly supports that the DUA of HC-24 has reached close to the maximum, that is, 1.

In an independent series of experiment, we also found that I_{pp} of HC-18-SL/G increases as the loaded amount of HC-18

(33) To obtain the average tilted angle of HC-*n* dyes in the silicalite-1 channels, we assumed that the long axes of the hemicyanine heads are tilted with an average specific angle θ from the channel direction after inclusion into the straight channels running perpendicular to the glass plane. d_{31} and d_{33} can then be expressed in terms of β_{HC-n} as eqs 4 and 5, respectively, by assuming that β_{HC-n} has only one dominant component $\beta = \beta_{\xi\xi\xi}$ along the long-axis direction ξ (the direction of linear dipole moment), and the microscopic local field correction *l* is independent of direction and frequency (sample is isotropic and dispersionless),

$$d_{33} = N\beta_{HC-n}\langle\cos^3\theta\rangle l^3/2 \tag{4}$$

$$d_{31} = N\beta_{HC-n}[\langle\cos\theta\rangle - \langle\cos^3\theta\rangle]l^3/4 \tag{5}$$

where *N* is the number density of HC-*n* (total number of HC-*n* within a unit volume, which is 1 cm × 1 cm × 400 nm in our case, see Table 1) and *l* is given by $(n^2 + 2)/3$, where *n* is the refractive index of zeolite which was estimated to be 1.48 (see text). The angle bracket indicates the orientational average of the molecules. Because HC-*n* dyes should have a very narrow distribution $f(\theta)$ of orientation, like $f(\theta) = s\delta(\theta - \theta_o)$, as a result of confinement within the narrow straight channels of silicalite-1, we have the following relationship (eq 6).

$$d_{33}/d_{31} = 2/\tan^2\theta = 109 \tag{6}$$

From the above equation, θ is derived to be 7.7.

(34) (a) Piccione, P. M.; Laberty, C.; Yang, S.; Camblor, M. A.; Navrotsky, A.; Davis, M. E. *J. Phys. Chem. B* **2000**, *104*, 10001−10011. (b) Eroshenko, V.; Regis, R.-C.; Soulard, M.; Patarin, J. *J. Am. Chem. Soc.* **2001**, *123*, 8129−8230.

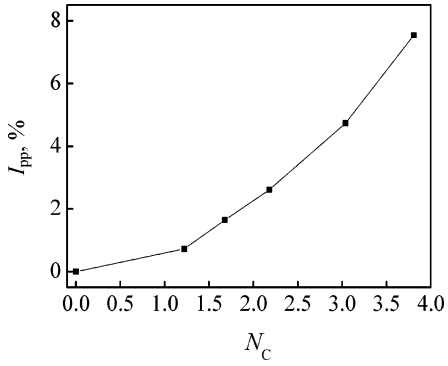

Figure 7. The parabolic relationship between N_c and the SHG intensity (I_{pp}) of HC-18-SL/G.

increases. Thus, the observed I_{pp} values were 0.7%, 1.6%, 2.6%, 4.7%, and 7.5% for N_C values of 1.2, 1.7, 2.2, 3.0, and 3.8,[35] respectively. The result is also graphically shown in Figure 7. As noticed, I_{pp} increases parabolically as N_C increases. Knowing the fact that SHG intensity is proportional to the square of the number density of the NLO dye, the above result indicates that HC-18 molecules enter the silicalite-1 channels with the same DUA regardless of the degree of loading.

The d_{33} value of HC-18-SL/G (5.3 pm V^{-1}) is more than 10 times larger than the d_{11} value of quartz (0.3 pm V^{-1}), or the d_{33} value of KDP ($\sim$3 pm V^{-1}), despite the fact that there are only 3.5 molecules in each channel. However, the observed d_{33} values are much smaller than those observed from LB films, which are in the range of 35 and 750 pm V^{-1}.[1,2,4−8] The reason for the d_{33} values of HC-*n*-SL/Gs being smaller than those of self-assembled molecular films is rather obvious considering the fact that the density of HC-*n* dyes in 400-nm thick silicalite-1 films is very small, in particular, for those of long chain HC-*n* dyes with high DUA values. For instance, in the case of HC-24-SL/G, N_C is essentially one. The comparison of the ratio of the volumes occupied by HC-24 in HC-24-SL/G and HC-18 in a LB film, that is, (1.35 nm^2 × 400 nm)/(0.42 nm^2 × 3.5 nm) = 367, with the ratio of the corresponding d_{33} values, 2.6/750 = 1/300, reveals that the lower d_{33} value of HC-24-SL/G originates from very low *N*. However, because the volume of each silicalite-1 channel does not change even after inclusion of larger numbers of HC-24 within each channel, we believe that our methodology bears a great potential to be developed into methods of preparing inorganic−organic composite NLO films with very high d_{33} values by developing methods of incorporating much larger numbers of HC-22 and HC-24 into the channels, perhaps by employing thicker silica zeolites with wider channels and uniform orientation. Furthermore, we found that HC-*n*-SL/Gs have long-term and high thermal and mechanical stabilities, which most of the LB and poled polymer NLO films are lacking.[1,2] For instance, we found that HC-*n*-SL/Gs retained their initial SHG activities even after keeping them in the atmosphere for 1 year or in an oven at 120 °C for 24 h, and even after rubbing the surface with fingers many times.

Unlike $AlPO_4$-5, ZSM-5, and Sb-SL powders loaded with PNA, the SL/Gs loaded with PNA by vapor phase inclusion (8%) did not exhibit SH activity, indicating the silicalite-1 channels have nearly the same affinities toward the nitro and the amino groups as was the case to pure silica ZSM-12.[21] This result therefore represents the first example that shows the symmetry breaking of a pure silica zeolite (free of Al or Sb) by aligned inclusion of a dipolar NLO dye.

It is also important to note that, in the case of the dye-loaded $AlPO_4$-5 crystals, the loading of the dyes into $AlPO_4$-5 should exceed certain thresholds such as 3% for PNA and 13% for MNA (by weight) for the composites to be SHG active. The requirement of concentration thresholds indicates that the NLO dyes have to undergo reorganization at high concentrations for them to produce a net bulk dipole moment.[14,15] In this respect, the fact that HC-*n*-SL/Gs (n = 22 and 24) exhibit SHG activities even with 0.1% loading (by weight) reveals the fact that the alignment of the dyes in the silcalite-1 channels is not a secondary phenomenon but is determined right from the beginning at the time of inclusion.

Overall, this report describes a method for the incorporation of a dipolar NLO dye (hemicyanine) with a high β value into a pure silica zeolite (silicalite-1) in high DUA by modification of the NLO dye. The successful demonstration of the use of zeolite films (rather than powders) as the inorganic hosts for the aligned inclusion of hemicyanine dyes verifies the great potential of the NLO-dye-including zeolites to be developed into practically viable SHG materials.

Acknowledgment. We thank the Ministry of Science and Technology (MOST) for supporting this work through the Creative Research Initiatives (CRI) program.

Supporting Information Available: Experimental tables and figures (PDF). This material is available free of charge via the Internet at http://pubs.acs.org.

JA037772Q

(35) The fact that this N_c value is higher than that shown in Table 1 is because SL/Gs were produced from a different batch.